
This is an electronic reprint of the original article.
This reprint *may differ from the original in pagination and typographic detail.*

Author(s): Trzcińska, A.; Piasecki, E.; Amar, A.; Czarnacki, W.; Keeley, N.; Kisielński, M.; Kliczewski, S.; Kowalczyk, M.; Lommel, B.; Mutterer, M.; Siudak, R.; Stolarz, A.; Strojek, I.; Tyurin, Grigory; Trzaska, Władysław

Title: Examination of the influence of transfer channels on the barrier height distribution:
Scattering of 20Ne on 58Ni, 60Ni, and 61Ni at near-barrier energies

Year: 2016

Version:

Please cite the original version:

Trzcińska, A., Piasecki, E., Amar, A., Czarnacki, W., Keeley, N., Kisielński, M., Kliczewski, S., Kowalczyk, M., Lommel, B., Mutterer, M., Siudak, R., Stolarz, A., Strojek, I., Tyurin, G., & Trzaska, W. (2016). Examination of the influence of transfer channels on the barrier height distribution: Scattering of 20Ne on 58Ni, 60Ni, and 61Ni at near-barrier energies. *Physical Review C*, 93(5), Article 054604.
<https://doi.org/10.1103/PhysRevC.93.054604>

All material supplied via JYX is protected by copyright and other intellectual property rights, and duplication or sale of all or part of any of the repository collections is not permitted, except that material may be duplicated by you for your research use or educational purposes in electronic or print form. You must obtain permission for any other use. Electronic or print copies may not be offered, whether for sale or otherwise to anyone who is not an authorised user.

Examination of the influence of transfer channels on the barrier height distribution: Scattering of ^{20}Ne on ^{58}Ni , ^{60}Ni , and ^{61}Ni at near-barrier energies

A. Trzcińska,^{1,*} E. Piasecki,^{1,2} A. Amar,³ W. Czarnacki,² N. Keeley,² M. Kisielński,^{1,2} S. Kliczewski,^{4,†} M. Kowalczyk,^{1,5} B. Lommel,⁶ M. Mutterer,^{6,7} R. Siudak,⁴ A. Stolarz,¹ I. Strojek,² G. Tiourin,⁸ and W. H. Trzaska⁸

¹Heavy Ion Laboratory, University of Warsaw, Warsaw, Poland

²National Centre for Nuclear Research, Otwock, Poland

³Physics Department, Faculty of Science, Tanta University, Tanta, Egypt

⁴The Henryk Niewodniczański Institute of Nuclear Physics Polish Academy of Sciences, Kraków, Poland

⁵Institute of Experimental Physics, University of Warsaw, Warsaw, Poland

⁶GSI Helmholtzzentrum für Schwerionenforschung GmbH, Darmstadt, Germany

⁷Darmstadt University of Technology, Darmstadt, Germany

⁸Department of Physics, University of Jyväskylä, Jyväskylä, Finland

(Received 11 March 2016; published 5 May 2016)

Background: It was suggested that the shape of the barrier height distribution can be determined not only by strong reaction channels (collective excitations) but also by weak channels such as transfers and/or noncollective excitations.

Purpose: The study of the barrier height distributions for the $^{20}\text{Ne} + ^{58,60,61}\text{Ni}$ systems requires information on transfer cross sections at near-barrier energies.

Methods: A measurement of the cross sections for various transfer channels at a backward angle (142 degrees), at a near-barrier energy was performed. Identification of products was based on time-of-flight and $\Delta E-E$ methods. A measurement of the angular distribution of α stripping in the $^{20}\text{Ne} + ^{61}\text{Ni}$ system was performed using a gas $\Delta E-E$ telescope.

Results: For all three systems studied: $^{20}\text{Ne} + ^{58}\text{Ni}$, ^{60}Ni , and ^{61}Ni total (sum of all transfer channels) cross sections are similar and dominated by α stripping.

Conclusions: The results, as well as coupled reaction channel calculations, suggest that transfer is not responsible for smoothing the barrier height distribution in $^{20}\text{Ne} + ^{61}\text{Ni}$, supporting the hypothesis that barrier distribution shapes are influenced by noncollective excitations.

DOI: 10.1103/PhysRevC.93.054604

I. INTRODUCTION

It is well known that coupling of the relative motion of reaction participants to their collective excitations is an important factor in the dynamics of heavy-ion fusion at near-barrier energies [1–3]. However, weak but numerous noncollective channels may also influence the reaction.

By “weak” channels we mean transfers and noncollective excitations giving rise to dissipation of projectile kinetic energy. Presently, the only feasible approach for the treating the latter phenomenon is including statistical methods of quantum mechanics applying random matrix theory. The first success in using this model to describe the barrier height distribution was obtained in Ref. [4].

The influence of transfer channels (mainly neutrons) on fusion has been studied in many works, e.g., Refs. [1,5–41]. There are a few competing models of the influence of transfer on fusion. Most of them concern only one or two neutron transfers and do not treat the transfer of heavier particles (e.g., α) or more nucleons, whereas heavier particle transfers are much stronger in many cases, e.g., Refs. [42–44]. In Refs. [24,27] the role of transfer channels in the barrier

distribution (BD) is discussed and it was shown that they can influence its shape. However, only heavy systems with large transfer cross sections were analyzed.

Rachkov *et al.* [33] describe enhancement of the fusion cross section due to neutron transfer but they do not discuss the barrier height distribution. Moreover, their model is only valid for positive Q_{gg} values. In the cases studied by us ($^{20}\text{Ni} + ^{90,92}\text{Zr}$ and $^{20}\text{Ni} + ^{58,60,61}\text{Ni}$), the neutron transfer Q_{gg} values are negative.

In the model of Sargsyan *et al.* [32,38] the change in nuclear deformation due to transfer is taken into account. This effect can change the barrier height and cause fusion enhancement or hindrance. However, as discussed below, these effects are not important for the systems studied in this work.

II. MOTIVATION OF THE MEASUREMENT

In our previous work [42,43,45–49], barrier distributions for $^{20}\text{Ne} + ^{\text{nat}}\text{Ni}$, $^{90,92}\text{Zr}$, $^{112,116,118}\text{Sn}$, and ^{208}Pb were studied and a discrepancy between standard coupled channel (CC) calculation predictions and the experimental results was observed for ^{92}Zr , $^{112,116,118}\text{Sn}$, and ^{208}Pb . The influence of weakly coupled channels on the barrier distribution shape for the above systems has already been discussed [42,44]. In the ^{208}Pb case it was suggested that the transfer channels with relatively large cross sections (nearly 30 mb/sr at backward

* agniecha@slcj.uw.edu.pl

† Deceased on July 3, 2015.

angles) are good candidates for the BD smoothing. However, in the $^{20}\text{Ne} + ^{92}\text{Zr}$ system, transfer channels are much weaker ($\sim 4 \text{ mb/sr}$) than in $^{20}\text{Ne} + ^{208}\text{Pb}$. This is why in the ^{92}Zr case the noncollective excitations rather than transfers are probably responsible for the lack of structure in the BD. This hypothesis seems to be supported by the fact that, for $^{20}\text{Ne} + ^{90}\text{Zr}$, the barrier distribution has clearly visible structure, while the total transfer cross section is nearly the same as in the $^{20}\text{Ne} + ^{92}\text{Zr}$ case [42].

Continuing these studies we performed an experiment in which BDs were determined for ^{20}Ne nuclei interacting with three Ni isotopes: $^{58,60,61}\text{Ni}$ [50]. Because these isotopes differ in their single-particle-level densities, we expected that, similar to the ^{92}Zr case, the noncollective excitations could change the predicted “structured” shape of the barrier distribution for the isotope with high level density. To check whether transfer channels in these systems can also influence barrier height distributions, we performed the experiment reported in the present work: a comparison of differential transfer cross sections for $^{20}\text{Ne} + ^{58,60,61}\text{Ni}$ backscattering at a near-barrier energy.

III. EXPERIMENTAL SETUP

The ^{20}Ne beam of 51 MeV energy (corresponding to the minimum in the BD expected according to CC calculations [50]) with a resolution of 0.9 MeV (full width at half maximum, or FWHM) and $\sim 60 \text{ enA}$ intensity was delivered by the Warsaw U200-P Cyclotron. Isotopically enriched self-supporting targets of $^{58,60,61}\text{Ni}$ (enrichment: 99.92%, 99.79%, and 92.92%, respectively) of $\sim 100 \mu\text{g/cm}^2$ thickness were prepared at the Target Laboratories at GSI [51] and the University of Jyväskylä [52].

A schematic of the experimental setup is presented in Fig. 1. The time-of-flight (TOF) technique was applied to identify the mass of detected ions. The flight base was 760 mm. The “start” signal was given by a fast microchannel-plate (MCP) detector. The “stop” signal was generated by an array of four Si detectors (PIN diode type) of $20 \text{ mm} \times 20 \text{ mm}$ placed at 142° (which corresponds to 154° in the center-of-mass system). At energies just below the mean barrier height corresponding

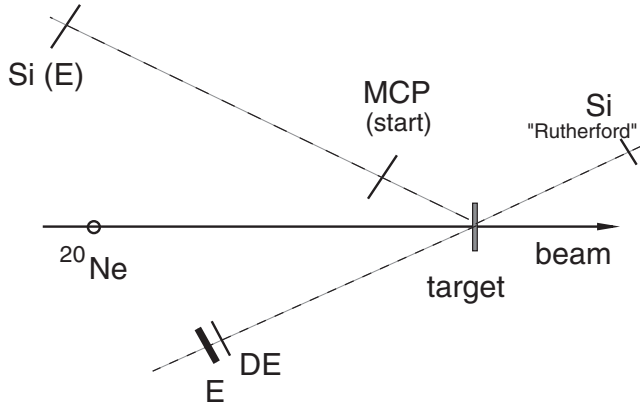


FIG. 1. Schematic view of experimental setup (a detailed description is given in the text).

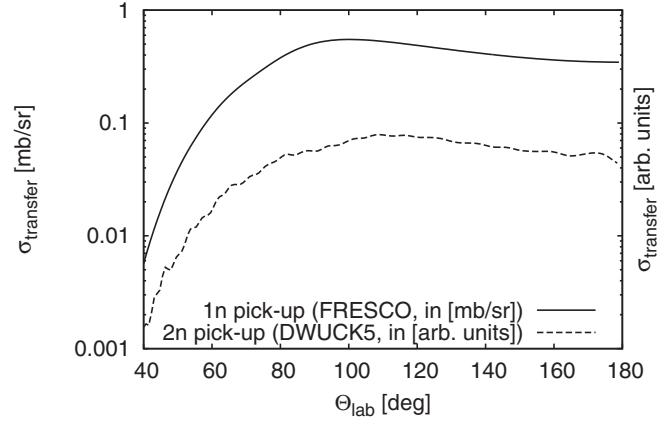


FIG. 2. Theoretical predictions of angular distribution of one- and two-neutron pickup for the $^{20}\text{Ne} + ^{61}\text{Ni}$ reaction at an energy of 51 MeV. For $1n$ pickup calculations were performed with the code FRESCO [53] (results in mb/sr), for $2n$ pick-up with DWUCK5 using the NRV system [54] (only pickup to the ground state was taken into account; the results are in arbitrary units because the spectroscopic factors are not known).

to the minimum seen in the BD for the ^{58}Ni target (see Fig. 4 in Ref. [50]), the transfer angular distribution has a flat maximum at backward angles, thus a measurement performed at 142° should give good information about the contributions of the different transfer channels. This expectation is confirmed by calculations of the neutron pickup (see Fig. 2) and the experimental results for the α stripping angular distribution (see Fig. 3).

For charge identification of scattered ions a $\Delta E - E$ telescope was employed. It was mounted on a movable arm of the ICARE detector system, which allowed the measurement of the angular distribution of the reaction products. The ΔE detector was a gas-filled-type (isobutane) detector with a thin ($2.5 \mu\text{m}$) mylar window, which ensured a low energy threshold. The residual energy was measured by a $300 \mu\text{m}$ Si E detector. Three Si detectors placed at 25° registered Rutherford-scattered ions and were used to check the beam energy.

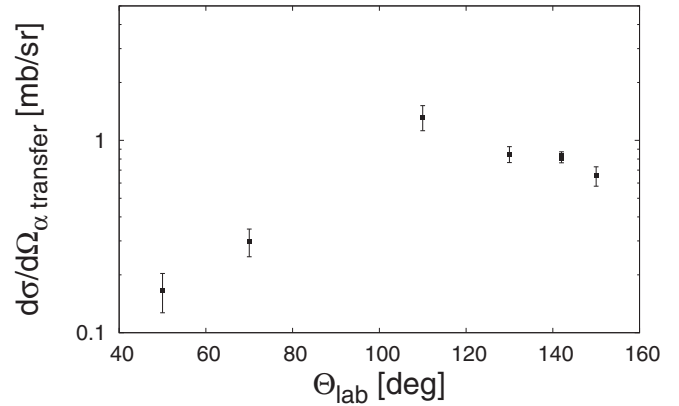


FIG. 3. Angular distribution of ^{16}O resulting from ^{20}Ne interacting with ^{61}Ni target at an energy $E_{\text{lab}} = 51 \text{ MeV}$ (experimental data).

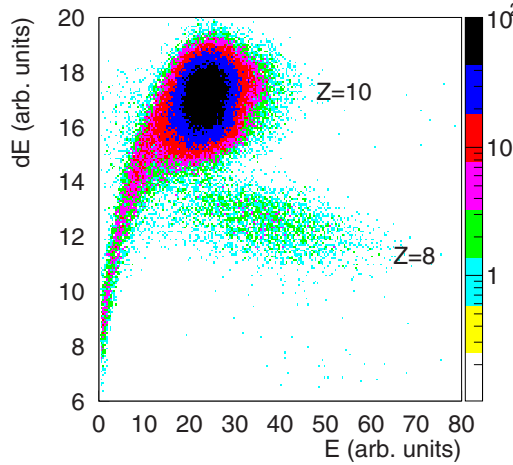


FIG. 4. The raw ΔE - E spectrum for $^{20}\text{Ne} + ^{61}\text{Ni}$ registered at 142° (in the laboratory system).

IV. DATA ANALYSIS AND RESULTS

The raw two-dimensional ΔE - E spectrum from a telescope placed at 142° for $^{20}\text{Ne} + ^{61}\text{Ni}$ is shown in Fig. 4. Only two groups of particles are seen: with atomic number $Z = 10$ and $Z = 8$. For other Ni targets the results look similar. In Fig. 3 the angular distribution of the $Z = 8$ ions, for $^{20}\text{Ne} + ^{61}\text{Ni}$, corresponding to α transfer, is presented.

The raw two-dimensional spectra (time of flight vs energy) of backscattered ions for the $^{20}\text{Ne} + ^{58,61}\text{Ni}$ systems are shown in Fig. 5 (in the ^{60}Ni case the spectrum looks like that for the ^{58}Ni target). In the interaction of ^{20}Ne with ^{58}Ni and ^{60}Ni , besides inelastic scattering, one observes only one transfer channel: that corresponding to $A = 16$ ions. For $^{20}\text{Ne} + ^{61}\text{Ni}$ other transfer channels are also present; namely, stripping of three nucleons (mass $A = 17$) as well as one- and two-nucleon pickup: ions with mass $A = 21$ and $A = 22$ [Fig. 5(b)].

Full product identification, i.e., mass and charge assignment, was made by combining the data from the two detectors described above and information on Q values. According to the Rehm systematics [55] there is a positive correlation between transfer probability and the effective Q value, Q_{eff} [56]. In Fig. 6 the Q_{gg} and Q_{eff} values are shown for the considered

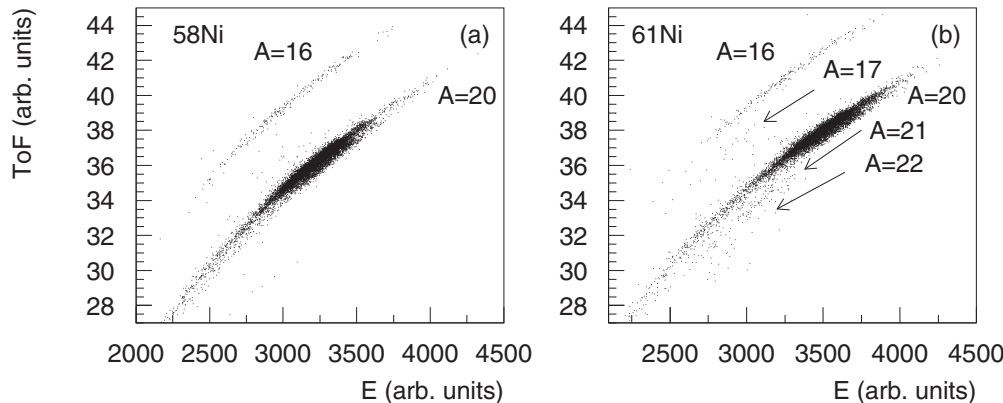


FIG. 5. The raw E -TOF results for (a) $^{20}\text{Ne} + ^{58}\text{Ni}$ and (b) $^{20}\text{Ne} + ^{61}\text{Ni}$ backscattered ions were registered at 142° (in the laboratory system).

transfer channels (i.e., resulting in $A = 22, 21, 17, 16$ and $Z = 10, 8$). It is seen that, e.g., $1n$ and $2n$ pickup are much more probable than $1p$ and $2p$ pickup, respectively, while for stripping reactions the situation is the reverse. Products with mass $A = 16$ are ^{16}O nuclei resulting from α stripping (high positive value of $Q_{\text{eff}} \sim 6$ MeV). Ions with mass $A = 21$ and $A = 22$ observed for ^{61}Ni are Ne isotopes produced in $1n$ and $2n$ pickup, respectively. We do not observe ^{21}Ne and ^{22}Ne in the interaction of ^{20}Ne with ^{58}Ni and ^{60}Ni because the Q_{eff} values for these cases are clearly more negative than for $^{20}\text{Ne} + ^{61}\text{Ni}$. Nuclei with $A = 17$ are most probably ^{17}O (produced with a positive value of Q_{eff} for $^{20}\text{Ne} + ^{61}\text{Ni}$).

Because the efficiency of the MCP detectors depends on several factors; namely, applied voltage and the charge (Z) and energy of the registered ions [57], in the analysis of spectra from the TOF system we also used information from the gas telescope which registered all particles with the same efficiency. We assumed that the efficiency of the MCP for ^{20}Ne , ^{21}Ne , and ^{22}Ne is the same, because these particles have the same charge and similar energies. For the oxygen ions the correction for MCP efficiency was determined by a comparison of the ratios of oxygen ion counts [$N(Z = 10)$] to neon ones [$N(Z = 8)$] registered by the TOF system and the gas-telescope:

$$\epsilon = \frac{N(Z = 8)^{\text{TOF}}}{N(Z = 10)^{\text{TOF}}} \Big/ \frac{N(Z = 8)^{\text{tel}}}{N(Z = 10)^{\text{tel}}}.$$

Based on the product identification described above, the contributions of one- and two-neutron pickup as well as α and $2p + 1n$ stripping to all registered backscattering events, σ_{tr}/σ_{QE} , were determined. Obviously, transfer contributions thus obtained are insensitive to uncertainties concerning the target thickness, beam intensity, and detection solid angles. The results are presented in Fig. 7(a).

The transfer cross sections σ_{tr} were calculated by using the formula

$$\sigma_{tr} = \frac{\sigma_{tr}}{\sigma_{QE}} \frac{\sigma_{QE}}{\sigma_{\text{Ruth}}} \sigma_{\text{Ruth}}, \quad (1)$$

where σ_{Ruth} is the calculated Rutherford cross section, the ratios $\sigma_{QE}/\sigma_{\text{Ruth}}$ were determined experimentally and for the beam energy of 51 MeV were equal to 0.71, 0.67, and 0.65 for

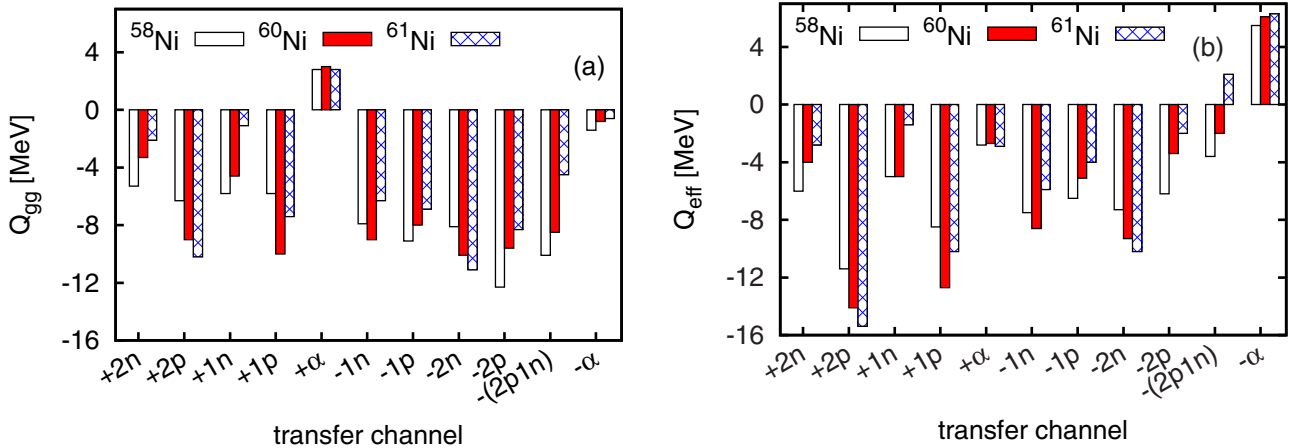


FIG. 6. (a) Q_{gg} and (b) Q_{eff} values for possible transfer channels in the $^{20}\text{Ne} + ^{58,60,61}\text{Ni}$ systems leading to products with masses observed in the experiment.

^{58}Ni , ^{60}Ni , and ^{61}Ni targets, respectively (see Ref. [50]). The ratios σ_{tr}/σ_{QE} were obtained as described above.

The resulting transfer-product cross sections are given in Table I and presented in Fig. 7(b).

The total (summed over all transfer channels) differential transfer cross sections obtained are similar for all three systems. Moreover, they are about three times smaller than the total transfer cross section for the $^{20}\text{Ne} + ^{90}\text{Zr}$ system, for which the QE barrier height distribution has a clearly visible structure (two maxima) [42]. These results support the hypothesis that transfer channels are not responsible for smoothing out the shape of the BD in the ^{61}Ni case.

V. DISCUSSION

The influence of transfer channels on the fusion cross section and particularly on the barrier height distribution is not well known. In Ref. [32] neutron-pair transfer in the sub-barrier capture process is analyzed. Since after the transfer the mass number and the deformation parameters of the interacting nuclei and, correspondingly, the height of the Coulomb barrier change, one might expect an enhancement or suppression

of the fusion cross section. In our case this effect is rather irrelevant, because the Ni and Zr nuclei are not deformed and the BD shapes according to the CC calculations are determined mainly by the ^{20}Ne deformation. Moreover, after possible (although rare) $2n$ pickup, the ^{22}Ni nucleus is also strongly deformed and, according to the CC calculations, structure should be visible in the BD [47,48].

The influence of transfer channels on barrier height distribution was analyzed in Refs. [24,27], but only heavy systems with high transfer cross sections were studied in these papers. In the cases studied by us, the neutron transfers account for only a small part of the scattering events (less than 1% in the ^{61}Ni and $^{90,92}\text{Zr}$ cases; see Figs. 7 and 4 of Ref. [42]). The most probable (but also rare) are alpha transfers: a few percent with a very small cross section: 0.8 mb/sr, 3.0 mb/sr, 2.1 mb/sr for Ni, ^{90}Zr , and ^{92}Zr , respectively. Since for the $^{20}\text{Ne} + ^{90}\text{Zr}$ system the BD is structured, the results for Ni (with clearly lower transfer cross section) rather exclude the transfer channels as the reason for the smoothing of the barrier height distribution observed in $^{20}\text{Ne} + ^{61}\text{Ni}$ [50].

Detailed theoretical checking of this conclusion is not possible at present. Accurate modeling of the effect of transfers

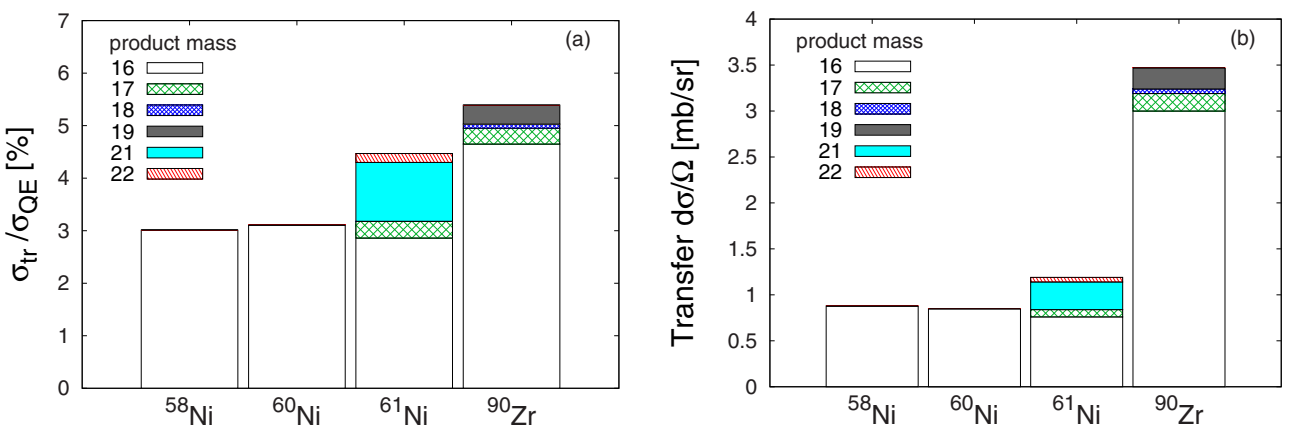


FIG. 7. (a) Contributions of different transfer channels to the quasi-elastic scattering at 142° in the laboratory system and (b) the corresponding differential cross sections for $^{20}\text{Ne} + ^{58,60,61}\text{Ni}$. Data for $^{20}\text{Ne} + ^{90}\text{Zr}$ at $E_{cms} \approx 51$ MeV [42] are also shown.

TABLE I. Transfer cross sections in the $^{20}\text{Ne} + {}^A\text{Ni}$ systems at $\Theta = 142^\circ$ for the near-barrier energy 51 MeV.

Target	Transfer product cross sections [mb/sr]			
	$A = 16$	$A = 17$	$A = 21$	$A = 22$
${}^{58}\text{Ni}$	0.88 ± 0.01	<0.01	<0.04	<0.03
${}^{60}\text{Ni}$	0.85 ± 0.01	<0.06	<0.09	<0.03
${}^{61}\text{Ni}$	0.76 ± 0.08	0.08 ± 0.02	0.30 ± 0.04	0.05 ± 0.01

of more than one nucleon, in particular α -particle transfers, is hampered by the lack of reliable absolute spectroscopic amplitudes for these processes.

However, in our case the situation is particular: as we mentioned before, for the ${}^{58,60}\text{Ni}$ targets the BD structure is observed, while for ${}^{61}\text{Ni}$ the structure it is smoothed out [50], whereas the α -particle-transfer cross sections for all three targets are almost the same (Fig. 7). This strongly suggests that the smoothing is not caused by α transfer. Moreover, as one can see from the figure, the main difference between the transfers for these three targets consists in the $1n$ pickup observed in the case of the ${}^{61}\text{Ni}$ target. Is this transfer responsible for smoothing? This possibility could be checked by calculations.

A series of coupled reaction channel (CRC) calculations was carried out with the code FRESCO [53] to investigate the influence of coupling of the single-neutron pickup reaction to backscattering. Inelastic excitation of the ${}^{20}\text{Ne} 2_1^+$ and 4_1^+ states, assumed to be members of a rotational band built on the 0^+ ground state, was also included in the calculations since these couplings are mainly responsible for the split in the calculated barrier distribution. The entrance channel optical potential was of Woods–Saxon form, with parameters $V = 57.23$ MeV, $R_0 = 1.15(A_p^{1/3} + A_t^{1/3})$ fm, $a_0 = 0.642$ fm, $W = 20$ MeV, $R_W = 1.0(A_p^{1/3} + A_t^{1/3})$ fm, and $a_W = 0.4$ fm (where A_p and A_t are projectile and target mass numbers, respectively). The parameter values for the real part of the potential were taken from Akyüz and Winther [58] with R_0 slightly adjusted in order to reproduce the mean barrier height [50]. An “interior” imaginary potential (also used in our previous work) simulates the ingoing-wave boundary condition.

The ${}^{20}\text{Ne}$ $B(E2)$ and $B(E4)$ values were 135.6 $e^2 \text{ fm}^4$ and 5265 $e^2 \text{ fm}^8$, respectively, taken from Ref. [59]. The corresponding nuclear deformation lengths were $\delta_2 = 1.436$ fm and $\delta_4 = 0.843$ fm.

To simplify the calculations, the ${}^{61}\text{Ni}$ nucleus was assumed inert. This is justified by the fact that collective excitation

TABLE II. States in ${}^{60}\text{Ni}$ coupled to in the CRC calculations.

E_x (MeV)	I^π	$C^2 S$
0.00	0^+	0.32
1.33	2^+	0.43
2.51	4^+	0.39
2.63	3^+	0.60

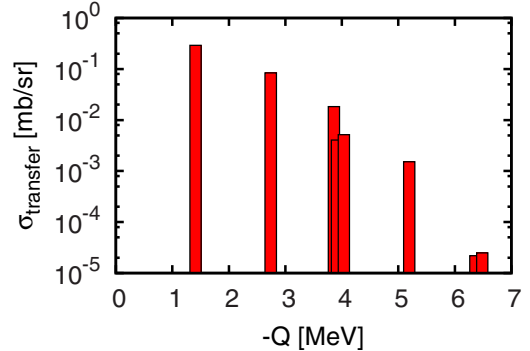


FIG. 8. The Q spectrum calculated for 51 MeV ${}^{20}\text{Ne}$ on ${}^{61}\text{Ni}$. See details in the text.

effects are dominated by ${}^{20}\text{Ne}$ due to the strong projectile deformation.

Spectroscopic factors for the ${}^{20}\text{Ne} \rightarrow {}^{21}\text{Ne}$ transitions were taken from Fortier *et al.* [60]. Pickup to the 0.35 MeV $5/2^+$ and 2.80 MeV $1/2^+$ states of ${}^{21}\text{Ne}$ was included, because these are the strongest individual single-neutron states. Transitions to the states in ${}^{60}\text{Ni}$ listed in Table II were included, with spectroscopic factors taken from Table IV of Ref. [61].

The $n + {}^{20}\text{Ne}$ and $n + {}^{60}\text{Ni}$ binding potentials were both of Woods–Saxon form with parameters $R_0 = 1.25A_c^{1/3}$ fm, $a_0 = 0.65$ fm, where A_c denotes the mass number of the corresponding “core” nucleus, the depths being adjusted to give the correct binding energies. The exit channel ${}^{21}\text{Ne} + {}^{60}\text{Ni}$ optical potential used the same parameters as the entrance channel potential. The full complex remnant term and nonorthogonality correction were included.

In Fig. 8 the Q spectrum obtained in the calculations is presented: the differential cross section at $\theta_{\text{lab}} = 142$ degrees plotted as a function of $Q = Q_{gg} - E_{ex}$, for 51 MeV ${}^{20}\text{Ne}$ on ${}^{61}\text{Ni}$. It shows the population of pairs of states in ${}^{21}\text{Ne}$ and ${}^{60}\text{Ni}$ by the ${}^{61}\text{Ni}({}^{20}\text{Ne}, {}^{21}\text{Ne}){}^{60}\text{Ni}$ one-neutron pickup.

The calculated barrier distributions are shown in Fig. 9. It is seen that the influence of $1n$ pickup is negligible. In particular it does not smooth the BD for the considered system. A similar

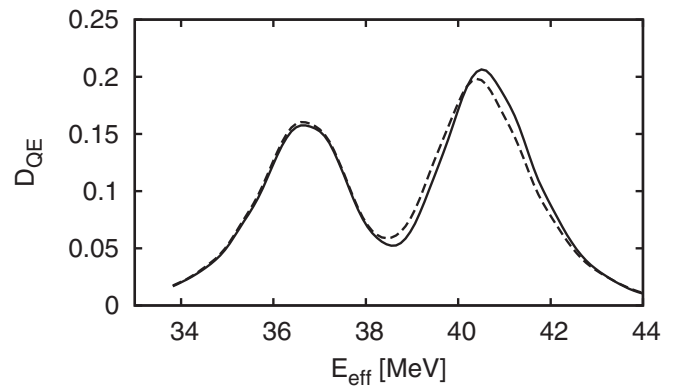


FIG. 9. Barrier height distribution calculated with the FRESCO code. Solid line is for only collective channels taken into account, dashed line is for $1n$ transfer also included.

conclusion (for $1p$ transfer in the $^{16}\text{O} + ^{144}\text{Sm}$ system) was presented in Ref. [62].

VI. SUMMARY AND CONCLUSIONS

Transfer cross sections have been measured for ^{20}Ne backscattering from $^{58,60,61}\text{Ni}$. The α transfer dominates ($\sim 0.9 \text{ mb/sr}$ at 142 degrees in the laboratory frame) and is very similar for all three targets. The sum of the differential cross sections for all observed transfer channels for each system studied is small and similar ($\sim 1 \text{ mb/sr}$). This observation, supported by CRC calculations, leads to the conclusion that smoothing of the BD shape in the ^{61}Ni case is not caused

by transfer reaction channels. This confirms the conclusion of Ref. [50] that the smoothing is most probably caused by noncollective excitations of the target.

ACKNOWLEDGMENTS

We wish to thank the Warsaw Cyclotron staff for the excellent beam provided. The authors are grateful to Raimo Seppälä for help in preparation of part of the targets at the Department of Physics, University of Jyväskylä, Finland. This work was partly supported by the National Science Centre, (Poland) under Contracts No. UMO-2013/08/M/ST2/00257 and UMO-2014/14/M/ST2/00738. This research was supported in part by the PL-Grid Infrastructure.

-
- [1] M. Dasgupta, D. J. Hinde, N. Rowley, and A. M. Stefanini, *Annu. Rev. Nucl. Part. Sci.* **48**, 401 (1998).
 - [2] K. Hagino and N. Takigawa, *Prog. Theor. Phys.* **128**, 1061 (2012).
 - [3] B. Back, H. Esbensen, C. Jiang, and K. Rehm, *Rev. Mod. Phys.* **86**, 317 (2014).
 - [4] S. Yusa, K. Hagino, and N. Rowley, *Phys. Rev. C* **88**, 054621 (2013).
 - [5] J. R. Leigh, *J. Phys. G* **23**, 1157 (1997).
 - [6] A. A. Sonzogni, J. D. Bierman, M. P. Kelly, J. P. Lestone, J. F. Liang, and R. Vandenbosch, *Phys. Rev. C* **57**, 722 (1998).
 - [7] O. A. Capurro, J. E. Testoni, D. Abriola, D. E. DiGregorio, G. V. Marti, A. J. Pacheco, and M. R. Spinella, *Phys. Rev. C* **61**, 037603 (2000).
 - [8] A. M. Stefanini, L. Corradi, A. M. Vinodkumar, Y. Feng, F. Scarlassara, G. Montagnoli, S. Beghini, and M. Bisogno, *Phys. Rev. C* **62**, 014601 (2000).
 - [9] V. Tripathi, L. T. Baby, J. J. Das, P. Sugathan, N. Madhavan, A. K. Sinha, P. V. Madhusudhana Rao, S. K. Hui, R. Singh, and K. Hagino, *Phys. Rev. C* **65**, 014614 (2001).
 - [10] A. Shrivastava, S. Kailas, A. Chatterjee, A. Navin, A. M. Samant, P. Singh, S. Santra, K. Mahata, B. S. Tomar, and G. Pollaro, *Phys. Rev. C* **63**, 054602 (2001).
 - [11] S. Sinha, M. R. Pahlavani, R. Varma, R. K. Choudhury, B. K. Nayak, and A. Saxena, *Phys. Rev. C* **64**, 024607 (2001).
 - [12] T. Schuck, H. Timmers, and M. Dasgupta, *Nucl. Phys. A* **712**, 14 (2002).
 - [13] G. Montagnoli, S. Beghini, F. Scarlassara, A. M. Stefanini, L. Corradi, C. Lin, G. Pollaro, and A. Winther, *Eur. Phys. J. A* **15**, 351 (2002).
 - [14] O. A. Capurro, J. E. Testoni, D. Abriola, D. E. DiGregorio, J. O. Fernandez Niello, G. V. Marti, A. J. Pacheco, M. R. Spinella, M. Ramirez, C. Balpardo, and M. Ortega, *Phys. Rev. C* **65**, 064617 (2002).
 - [15] R. Simoes, D. Monteiro, L. Ono, A. Jacob, J. Shorto, N. Added, and E. Crema, *Phys. Lett. B* **527**, 187 (2002).
 - [16] A. Mukherjee, M. Dasgupta, D. J. Hinde, K. Hagino, J. R. Leigh, J. C. Mein, C. R. Morton, J. O. Newton, and H. Timmers, *Phys. Rev. C* **66**, 034607 (2002).
 - [17] V. I. Zagrebaev, *Phys. Rev. C* **67**, 061601(R) (2003).
 - [18] D. Monteiro, R. Simoes, J. Shorto, A. Jacob, L. Ono, L. Paulucci, N. Added, and E. Crema, *Nucl. Phys. A* **725**, 60 (2003).
 - [19] A. M. Stefanini, F. Scarlassara, S. Beghini, G. Montagnoli, R. Silvestri, M. Trotta, B. R. Behera, L. Corradi, E. Fioretto, A. Gadea, Y. W. Wu, S. Szilner, H. Q. Zhang, Z. H. Liu, M. Ruan, F. Yang, and N. Rowley, *Phys. Rev. C* **73**, 034606 (2006).
 - [20] N. Keeley and N. Alamanos, *Phys. Rev. C* **75**, 054610 (2007).
 - [21] A. M. Stefanini, B. R. Behera, S. Beghini, L. Corradi, E. Fioretto, A. Gadea, G. Montagnoli, N. Rowley, F. Scarlassara, S. Szilner, and M. Trotta, *Phys. Rev. C* **76**, 014610 (2007).
 - [22] C. Lin, H. Zhang, F. Yang, M. Ruan, Z. Liu, Y. Wu, X. Wu, P. Zhou, C. Zhang, G. Zhang, G. An, H. Jia, and X. Xu, *Nucl. Phys. A* **787**, 281c (2007).
 - [23] F. Yang, C. J. Lin, X. K. Wu, H. Q. Zhang, C. L. Zhang, P. Zhou, and Z. H. Liu, *Phys. Rev. C* **77**, 014601 (2008).
 - [24] G. Pollaro, *Phys. Rev. Lett.* **100**, 252701 (2008).
 - [25] N. Keeley, *Phys. Rev. C* **80**, 064614 (2009).
 - [26] H. Q. Zhang, C. J. Lin, F. Yang, H. M. Jia, X. X. Xu, Z. D. Wu, F. Jia, S. T. Zhang, Z. H. Liu, A. Richard, and C. Beck, *Phys. Rev. C* **82**, 054609 (2010).
 - [27] G. Pollaro, *Nucl. Phys. A* **834**, 139c (2010).
 - [28] Z. Kohley, J. F. Liang, D. Shapira, R. L. Varner, C. J. Gross, J. M. Allmond, A. L. Caraley, E. A. Coello, F. Favela, K. Lagergren, and P. E. Mueller, *Phys. Rev. Lett.* **107**, 202701 (2011).
 - [29] M. Evers, M. Dasgupta, D. J. Hinde, D. H. Luong, R. Rafiei, R. du Rietz, and C. Simenel, *Phys. Rev. C* **84**, 054614 (2011).
 - [30] V. V. Sargsyan, G. G. Adamian, N. V. Antonenko, W. Scheid, and H. Q. Zhang, *Phys. Rev. C* **84**, 064614 (2011).
 - [31] F. Scarlassara, G. Montagnoli, E. Fioretto, C. Jiang, A. M. Stefanini, L. Corradi, B. Back, N. Patel, K. Rehm, D. Seweryniak, P. P. Singh, X. Tang, C. Deibel, B. D. Giovine, J. Greene, H. Henderson, M. Notani, S. Marley, and S. Zhu, *EPL Web Conf.* **17**, 05002 (2011).
 - [32] V. V. Sargsyan, G. Scamps, G. G. Adamian, N. V. Antonenko, and D. Lacroix, *Phys. Rev. C* **88**, 064601 (2013).
 - [33] V. A. Rachkov, A. V. Karpov, A. S. Denikin, and V. I. Zagrebaev, *Phys. Rev. C* **90**, 014614 (2014).
 - [34] H. M. Jia, C. J. Lin, F. Yang, X. X. Xu, H. Q. Zhang, Z. H. Liu, Z. D. Wu, L. Yang, N. R. Ma, P. F. Bao, and L. J. Sun, *Phys. Rev. C* **89**, 064605 (2014).
 - [35] D. Montanari, L. Corradi, S. Szilner, G. Pollaro, E. Fioretto, G. Montagnoli, F. Scarlassara, A. M. Stefanini, S. Courtin, A. Goasdoué, F. Haas, D. Jelavić Malenica, C. Michelagnoli, T. Mijatović, N. Soić, C. A. Ur, and M. VargaPajtler, *Phys. Rev. Lett.* **113**, 052501 (2014).

- [36] M. S. Gautam, *Phys. Rev. C* **90**, 024620 (2014).
- [37] A. A. Ogloblin, H. Q. Zhang, C. J. Lin, H. M. Jia, S. V. Khlebnikov, E. A. Kuzmin, W. H. Trzaska, X. X. Xu, F. Yan, V. V. Sargsyan, G. G. Adamian, N. V. Antonenko, and W. Scheid, *Eur. Phys. J. A* **50**, 157 (2014).
- [38] V. V. Sargsyan, G. G. Adamian, N. V. Antonenko, W. Scheid, and H. Q. Zhang, *Phys. Rev. C* **91**, 014613 (2015).
- [39] A. V. Karpov, V. A. Rachkov, and V. V. Samarin, *Phys. Rev. C* **92**, 064603 (2015).
- [40] G. Scamps and K. Hagino, *Phys. Rev. C* **92**, 054614 (2015).
- [41] K. Hagino and G. Scamps, *Phys. Rev. C* **92**, 064602 (2015).
- [42] E. Piasecki, Ł. Świderski, W. Gawlikowicz, J. Jastrzębski, N. Keeley, M. Kisielński, S. Kliczewski, A. Kordyasz, M. Kowalczyk, S. Khlebnikov, E. Koshchii, E. Kozulin, T. Krogulski, T. Loktev, M. Mutterer, K. Piasecki, A. Piórkowska, K. Rusek, A. Staudt, M. Sillanpää, S. Smirnov, I. Strojek, G. Tiourin, W. H. Trzaska, A. Trzcińska, K. Hagino, and N. Rowley, *Phys. Rev. C* **80**, 054613 (2009).
- [43] E. Piasecki, Ł. Świderski, N. Keeley, M. Kisielński, M. Kowalczyk, S. Khlebnikov, T. Krogulski, K. Piasecki, G. Tiourin, M. Sillanpää, W. H. Trzaska, and A. Trzcińska, *Phys. Rev. C* **85**, 054608 (2012).
- [44] E. Piasecki, W. Czarnacki, N. Keeley, M. Kisielński, S. Kliczewski, A. Kordyasz, M. Kowalczyk, S. Khlebnikov, E. Koshchii, T. Krogulski, T. Loktev, M. Mutterer, A. Piórkowska, K. Rusek, M. Sillanpää, A. Staudt, I. Strojek, S. Smirnov, W. H. Trzaska, and A. Trzcińska, *Phys. Rev. C* **85**, 054604 (2012).
- [45] E. Piasecki, M. Kowalczyk, K. Piasecki, Ł. Świderski, J. Srebrny, M. Witecki, F. Carstoiu, W. Czarnacki, K. Rusek, J. Iwanicki, J. Jastrzębski, M. Kisielński, A. Kordyasz, A. Stolarz, J. Tys, T. Krogulski, and N. Rowley, *Phys. Rev. C* **65**, 054611 (2002).
- [46] L. Świderski, P. Czosnyka, M. Kowalczyk, E. Piasecki, K. Piasecki, M. Witecki, J. Jastrzebski, A. Kordyasz, M. Kisielinski, T. Krogulski, N. Rowley, C. Marchetta, A. Pagano, M. Mutterer, W. H. Trzaska, and K. Hagino, *Int. J. Mod. Phys. E* **E13**, 315 (2004).
- [47] E. Piasecki, Ł. Świderski, P. Czosnyka, M. Kowalczyk, K. Piasecki, M. Witecki, T. Czosnyka, J. Jastrzębski, A. Kordyasz, M. Kisielński, T. Krogulski, M. Mutterer, S. Khlebnikov, W. Trzaska, K. Hagino, and N. Rowley, *Phys. Lett. B* **615**, 55 (2005).
- [48] L. Świderski, E. Piasecki, P. Czosnyka, T. Krogulski, and N. Rowley, *Int. J. Mod. Phys. E* **14**, 341 (2005).
- [49] E. Piasecki, M. Kowalczyk, J. Jastrze?bski, T. Krogulski, K. Piasecki, K. Rusek, Ł. Świderski, S. Khlebnikov, M. Mutterer, W. H. Trzaska, M. Sillanpää, S. Smirnov, G. Tiourin, S. Dmitriev, E. Kozulin, A. Ogloblin, and N. Rowley, in *Proc. Frontiers in Nuclear Structure, and Reactions (FINUSTAR 2)*, Crete, Greece, 10–14 September 2007, AIP Conf. Proc. Vol. 1012 (AIP, New York, 2008), pp. 238.
- [50] A. Trzcińska, E. Piasecki, K. Hagino, W. Czarnacki, P. Decowski, N. Keeley, M. Kisielński, P. Koczoń, A. Kordyasz, E. Koshchii, M. Kowalczyk, B. Lommel, A. Stolarz, I. Strojek, and K. Zerva, *Phys. Rev. C* **92**, 034619 (2015).
- [51] B. Lommel, W. Hartmann, A. Huebner, B. Kindler, and J. Steiner, *Nucl. Instrum. Methods Phys. Res., Sect. A* **655**, 44 (2011).
- [52] A. Stolarz and R. Seppälä, *J. Radioanal. Nucl. Chem.* **299**, 1133 (2013).
- [53] I. J. Thompson, *Comput. Phys. Rep.* **7**, 167 (1988).
- [54] V. Zagrebaev *et al.*, <http://nrv.jinr.ru>.
- [55] K. E. Rehm, C. Beck, A. van den Berg, D. G. Kovar, L. L. Lee, W. C. Ma, F. Videbaek, and T. F. Wang, *Phys. Rev. C* **42**, 2497 (1990).
- [56] R. Bass, *Nuclear Reactions with Heavy Ions* (Springer-Verlag, Berlin Heidelberg, 1980).
- [57] A. Musumara *et al.*, *Nucl. Instrum. Methods Phys. Res., Sect. A* **612**, 399 (2010).
- [58] O. Akyüz and A. Winther, in *Nuclear Structure and Heavy-Ion Collisions*, Proceedings of the International School of Physics ‘Enrico Fermi’, course LXXVII, Varenna on Lake Como, Villa Monastero, 9th–21st July 1979, edited by R. A. Broglia, R. A. Ricci, and C. H. Dasso (North-Holland, Oxford, 1981).
- [59] G. S. Blanpied, B. G. Ritchie, M. L. Barlett, R. W. Ferguson, G. W. Hoffmann, J. A. McGill, and B. H. Wildenthal, *Phys. Rev. C* **38**, 2180 (1988).
- [60] S. Fortier, S. Gales, S. M. Austin, W. Benenson, G. M. Crawley, C. Djalali, J. S. Winfield, and G. Yoo, *Phys. Rev. C* **41**, 2689 (1990).
- [61] D. H. Koang, W. S. Chien, and H. Rossner, *Phys. Rev. C* **13**, 1470 (1976).
- [62] F. M. Zamrun and K. Hagino, *Phys. Rev. C* **77**, 014606 (2008).